# A CONTACTLESS TECHNIQUE FOR MEASURING MINORITY-CARRIER PARAMETERS IN SILICON

*R.K. Ahrenkiel and S.W. Johnston*
*National Renewable Energy Laboratory*
*1617 Cole Blvd., Golden, Colorado 80401 USA*

## Introduction

Characterization of minority-carrier parameters is a primary interest for a range of devices, including solar cells. For "on-line" testing needs, contactless techniques are mandatory, as any diagnostic requiring contact formation is impractical. Here, we will describe the resonance-coupled photoconductive decay (RCPCD) technique that has proven to be a valuable diagnostic for a number of semiconductor technologies.

This technique avoids some of the inherent limitations of microwave reflection. Our system is a pump-probe technique, using an optical pump and a microwave probe (400 to 900 MHz). These low frequency microwaves penetrate most silicon wafers with common doping levels. By varying the optical excitation wavelength, one can probe wafers of standard (300 to 400 μm) wafer thickness. Also, the method is very linear in sample photoconductivity, and we have observed a linear response over more than three orders of magnitude of excess carrier concentration. This attribute allows us to measure the carrier recombination lifetime over many decades of injection level, allowing the use of a procedure that is called injection-level spectroscopy (ILS).

The RCPCD technique was developed[1,2,3,4,5,6] at the National Renewable Energy Laboratory (NREL) and has been applied to more than 5000 samples, ranging from small-area thin films to 350-μm-thick, 250-mm-diameter silicon wafers. In addition, the lifetimes in semiconductor ingots of irregular shape have been successfully measured as no particular size or shape is required for the RCPCD analysis.

## Theory of the Detection Process

A schematic representation of the apparatus is shown in Fig. 1. The sample is coupled to the electromagnetic field of a small antenna, a several-turn loop plus a rectangular copper box that is open on one end. The sample lies on an insulating, moveable platform, and the antenna configuration directs the microwave energy toward the box opening. The antenna-sample behave like an antenna array with active and passive elements. The antenna-sample coupling is commonly called impedance coupling. The complex impedance of the antenna can be described as a combination of radiation resistance and inductive reactance in this configuration. The antenna is placed in parallel with a small variable capacitor, and the two elements produce a circuit with a high quality factor (i.e. Q) at the parallel resonance of the circuit. When the semiconducting sample is coupled to the antenna, the mutual impedance modifies the input impedance of the antenna. We write the coupled impedance, $Z_{in}$, looking into the antenna terminals, as:

$$z_{in} = Z_{ant} - \frac{Z_{12}^2}{Z_s} \quad . \qquad (1)$$

Here, $Z_{ant}$ is the impedance of the isolated antenna, and $Z_{12}$ is the mutual impedance. The quantity $Z_s$ is the high-frequency impedance of the sample and depends on sample size and conductivity. The mutual impedance depends primarily on the antenna-sample spacing, but it also depends on the sample size and conductivity. In operation, the antenna-sample spacing is varied until a predetermined impedance is presented as the antenna input. The spacing varies from several centimeters for large wafers to a few mm for small-area thin films. Small changes in coupled reactance, produced by variable sample size, is accommodated by small adjustments in the parallel capacitor.

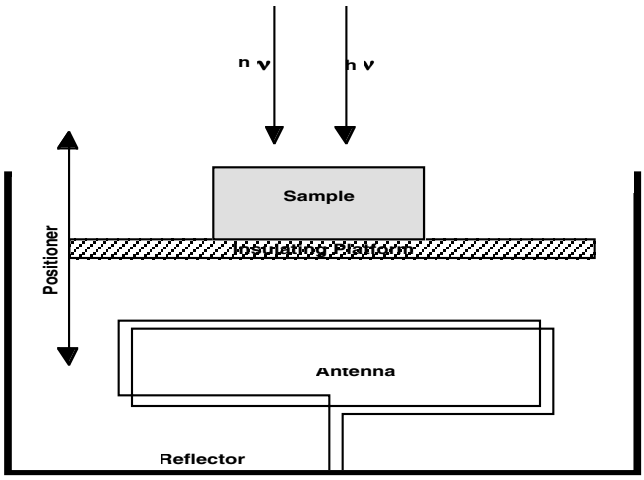


Fig. 1. Schematic of the samples chamber showing the relative positions of sample and antenna.

The antenna impedance, $Z_{in}$, is adjusted to match the input of a unidirectional coupler, usually 50 ohms. This is done by adjusting the sample positioner until the output of the coupler shows a null. The unidirectional coupler output is amplified by wide-bandwidth ac amplifiers, and then input to a high-frequency mixer module. This signal is mixed with a signal taken from the antenna driver circuit after the two signals are phase-matched. In operation, we use the dc component of the mixer output, and run that component through a wide-bandwidth dc amplifier before displaying the photoconductivity signal on an oscilloscope. The 2ω component has also been used (where ω is the oscillator frequency) to process the transient photoconductivity.

We can write the input impedance of the system under pulsed excitation as:

$$z_{in} = Z_{ant} - Z_{12}^2 [\sigma_s + \Delta\sigma_s(t)]. \quad (2)$$

Here, $\sigma_s$ is the dark conductance of the sample, and $\Delta\sigma(t)$ is the pulsed photoconductivity of the sample. One can use pulse excitation energies such that: $\Delta\sigma_s(t) >> \sigma_s$, and a linear response is still observed. To provide for the desired linearity and large dynamic range for $\Delta\sigma(t)$, we adjust $Z_{12} << Z_{ant}$. The photoconductive signal is then connected to a digitizing oscilloscope, where the signal voltage is:

$$V(t) = AZ_{12}^2 \Delta\sigma_s(t) . \quad (3)$$

Here, A is the overall system gain and is 40 dB or more in our current apparatus.

The system, as shown, is sensitive to the movement of laboratory personnel in the room, as well as room lighting. To shield the apparatus from these disturbances, we enclose the entire sensor apparatus in a much larger conducting enclosure that is a resonant cavity at near the antenna resonant frequency. This enclosure does not degrade the signal and may, in fact, enhance the system sensitivity. The walls of the enclosure become nodes of the rf standing waves, and the sample is near an anti-node.

A variety of pulsed optical light sources have been used successfully with this system. These include xenon flash lamps and inexpensive light-emitting diodes. The sources of choice for research applications are YAG-pumped optical parametric oscillators (OPO), because these provide wide wavelength tunability for the variety of measurements that will be described here. The output intensities of these laser-based sources are usually much too large for most measurements, and they are reduced several orders of magnitude by calibrated neutral-density filters.

## Frequency Response

Our primary system was designed for operation at about 400 MHz. The system response is optimum at the range of 415 to 425 MHz. The dimensions of the exterior enclosure are 46 cm wide, 38 cm high, and 61 cm long. The data of Fig. 2 were obtained using 150-mm, electronic-grade silicon wafers, with a 100-A-thick thermal oxide grown on the front surface. An optical excitation pulse is supplied from the OPO pumped by a tripled YAG laser (Coherent Radiation Infinity system). The wavelength of the OPO was set at 1000 nm so that nearly uniform depth excitation is produced. The OPO beam was reduced in intensity with a neutral-density filter (OD=2), and the incident photon flux is about 5.5 x $10^{12}$ photons/cm$^2$. The system was run over a range of frequencies from about 410 MHz to 430 MHz, to find the optimum operating frequency.

These measurements were performed to find the optimum operating frequency. The first set was done with the system completely sealed by fastening the top lid on the exterior chamber. Figure 2, curve A, shows the peak photoresponse of the system with the 150-mm, electronic-grade silicon wafer in the sample holder. The excitation area of the pulse is about 1.0 cm$^2$ at the sample, and the injected excess-carrier density is about 1.4 x $10^{14}$ cm$^{-3}$. There is a peak in the response over the range of 415 to 420 MHz, which is the preferred operating frequency for these measurements. The system can be operated with the top of the exterior enclosure removed, but the open system is more susceptible to ambient electrical noise. Curve B shows the response to the same wafer, with the top removed and the enclosure open, and one sees a slightly lower response. However, this mode of operation is superior when one needs a very fast-turnaround measurement.

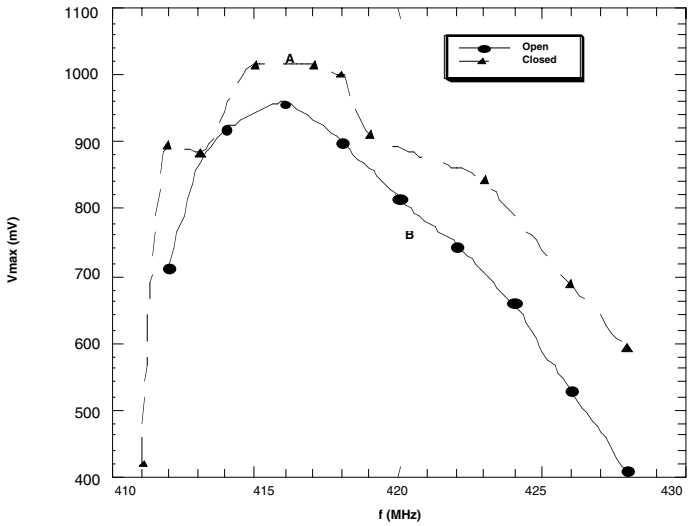


Fig. 2. System response for a 150 mm silicon wafer at a range of operating frequencies from 410 MHz to 430 MHz.

## Theory of Photoconductive Decay

This RCPCD technique measures the transient ambipolar photoconductivity $\Delta\sigma(t)$ following pulsed excitation, which can be written as:

$$\Delta\sigma = q(\mu_n + \mu_p)\rho(x,t). \quad (4)$$

Here, $\mu_n$ ($\mu_p$) are the electron (hole) mobilities, and $\rho(x,t)$ is the excess-carrier concentration. When recombination can be written in terms of a single lifetime, $\tau$, we can write Eqn. (5) as:

$$\Delta\sigma = q(\mu_n + \mu_p)\rho(x)\exp(-t/\tau). \quad (5)$$

If the incident pulse is monochromatic, the conductivity has the following form:

$$\Delta\sigma(t) = qI_0(\mu_n + \mu_p)(1-\exp-\{\alpha[\lambda]W\})\exp(-t/\tau). \quad (6)$$

Here, $\alpha(\lambda)$ is the absorption coefficient of the material, $I_0$ is the incident optical density in photons/cm$^2$, and W is the sample thickness. We measure the ac. photocurrent driven by the microwave electric field. The photocurrent density per unit of electric field is then:

$$j(\omega,t) = qI_0(\mu_n + \mu_p)[1-\exp(-\alpha W)]\exp(-t/\tau). \quad (\text{amp/cm}^2) \quad (7)$$

From this result, we see that the pulse height per photon is proportional to the mobility sum, $\mu_n + \mu_p$. The time-integrated photoconductivity at a fixed wavelength as:

$$Q(\lambda) = \int_0^{t_{max}} j(\omega,t)\, dt = qI_0[1-\exp(-\alpha W)]\tau(\mu_n+\mu_p). \quad (\text{amp/cm}^2) \quad (8)$$

Using the Einstein relationship, we can write Eqn. (8) as:

$$Q(\lambda) = \frac{q^2 I_0}{KT}\{1-\exp[(-\alpha(\lambda)L]\}(L_n^2 + L_p^2). \quad (9)$$

For wavelengths that are strongly absorbed ($\alpha W >> 1$), the integrated photoresponse is:

$$Q(\lambda) = \frac{q^2 I_0 L_a^2}{KT}, \quad (\text{Coulomb/volt}) \quad (10)$$

where $L_a \equiv \sqrt{L_n^2 + L_p^2}$, which is the root-mean-square diffusion length.

One can calibrate the data in terms of diffusion length.

## Injection-Level Spectroscopy

The SRH recombination rate produced by a single-point defect at energy $E_t$ in the forbidden gap is described by the well-known equation:

$$\frac{dn}{dt} = \frac{dp}{dt} = -\frac{\sigma_p \sigma_n v_{th} N_t[pn - n_i^2]}{\sigma_n\left[n + n_i e^{\frac{E_t - E_i}{kT}}\right] + \sigma_p\left[p + n_i e^{\frac{E_i - E_t}{kT}}\right]} \quad (11)$$

Here, n and p are the densities of free electrons and holes, respectively, and $N_t$ is the defect density; $\sigma_n$ and $\sigma_p$ are the capture cross-sections for electrons and holes, respectively. Also, $V_{th}$ is the thermal velocity, $n_i$ is the intrinsic density, and $E_i$ is the intrinsic energy. The SRH lifetime is not a single number, but a function of the electron and hole concentrations. The limits at low/high injection are:

$$\tau_{low} = \frac{1}{\sigma_n N_t v_{th}}.$$
$$\tau_{high} = \frac{1}{\sigma_p N_t v_{th}} + \frac{1}{\sigma_n N_t v_{th}} \quad (12)$$

The ratio of the high-injection to low-injection lifetime is:

$$\text{ratio} = \frac{\sigma_n + \sigma_p}{\sigma_p}. \tag{13}$$

This ratio is a number that is usually unique to an impurity and is the basis of injection-level spectroscopy.

A batch of Czochralski-grown wafers, that were provided by a commercial vendor, were doped with transition metals, and the lifetime was measured over about three orders of magnitude of injection level. The wafer thicknesses averaged about 330 μm, and the resistivity was p-type and about 100 ohm-cm. Several of the wafers were run in the as-received condition and then processed to reduce surface recombination. The wafers were etched in dilute HF etch to remove the native oxide. This was followed by a rinse in deionized water and submersion in a methanol solution containing iodine [7]. In Fig. 3, the RCPCD lifetime measurement was made in the iodine/methanol solution, and the surface recombinaton effect was essentially eliminated.

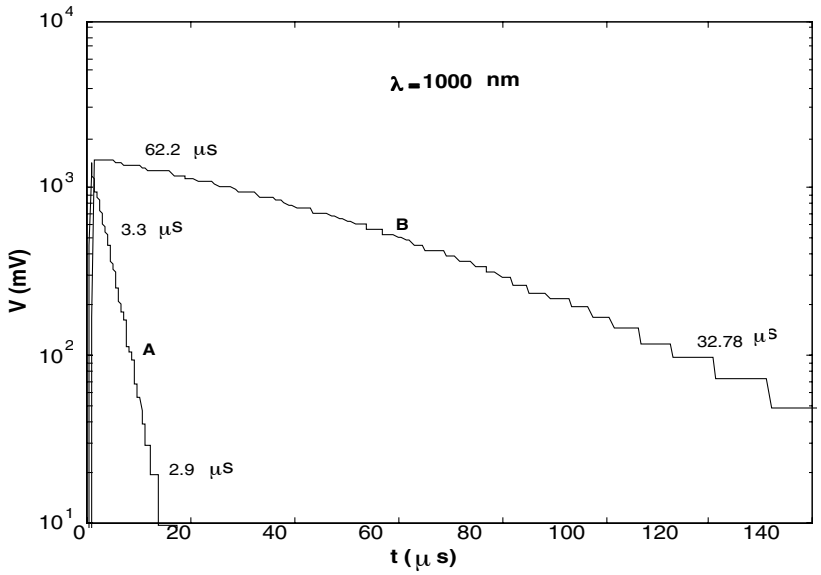


Fig. 3. RCPCD decay data for a Czochralski-grown wafer. A: As received from the vendor; B: After etching and while immersed in iodine/methanol solution.

Figure 4 shows the wafer measurement in air (curve A) and in iodine-methanol solution (curve B). Shown on curve A are the low- and high-injection lifetimes, respectively. Curve B shows that the lifetime increases over a factor of 10 when the surface is passivated. Assuming that S=0 for the treated wafers, the surface recombination velocity, S, is about 5.5 x $10^3$ cm/s and the bulk, low- and high-injections lifetime are about 33 μs and 62 μs, respectively. Figure 4 shows RCPCD data from another wafer from the same lot that was doped with iron. This wafer was not immersed in iodine/methanol solution to eliminate surface recombination. Metallic iron was electrodeposited on the surface, and the wafer was then furnace annealed at 800°C for several hours. Prior to these lifetime measurements, the wafers were heated to about 250°C and quenched in water. Curve A shows the RCPCD data for the wafer prior to iron doping. The low-injection lifetime was 12.5 μs, and the high-injection lifetime was 18.9 μs. After Fe doping and the water quench to produce interstitial Fe, the data of curves B and C were obtained. Digitizing error prevents good data collection at lower injection levels, but the wafer was rerun with an additional neutral density filter of 3.0. This reduces the incident flux by a factor of 1000, and the data of curve C were produced. Here, the lifetime drops to 1.17 μs. The injection ratio is calculated to be 17.

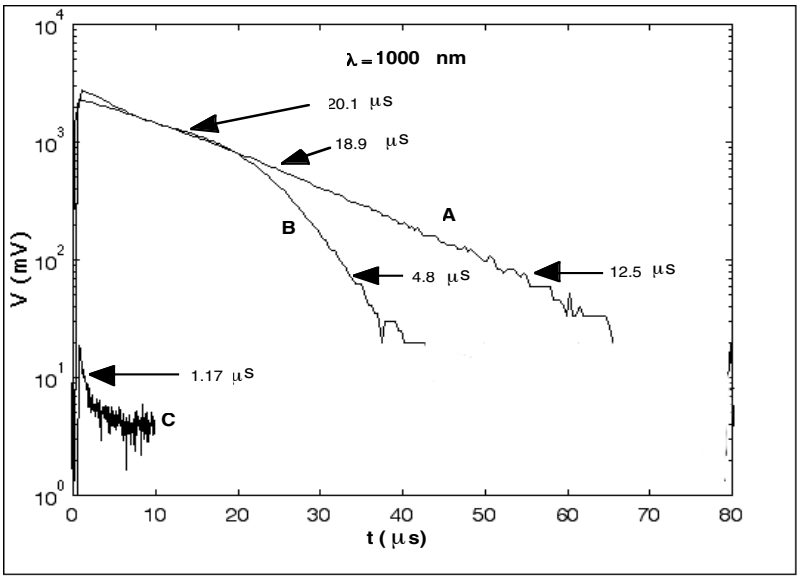


Fig. 4. RCPCD data for a Czochralski-grown wafer from the same lot as the wafer of Fig. 3. A: As received; B: Diffusion of Fe into wafer and at higher injection levels; C: The wafer of curve B, but at the lowest injection levels.

One could obtain more precise data using the iodine-methanol treatment on all wafers, and getting the lifetime ratio with the surface effects removed. We can also use the ratio of 17 as an indicator of interstitial Fe, when the surface is unpassivated.

## Summary

We have demonstrated the versatility of the contactless RCPCD technique for a variety of semiconductor measurements. Other information that can be obtained from RCPCD includes:

The spectral response of the semiconductor.
The specific sensitivity, S*, of the semiconductor or photoconduction[8].
The photoexcitation spectra (PES) gives the relative absorption coefficient, $\alpha$, of thin films.
The PES gives the absorption coeffficient of deep impurity levels.

Other successful measurements that were not included here are:

A lifetime depth profile by excitation wavelength variation.
A defect level energy determination by combining injection-level spectroscopy and variable sample temperature.

In summary, the RCPCD technique has been shown to be a very powerful, contactless method of semiconductor characterization.

## Acknowledgements

The authors would like to thank R. Bhattacharya for doing the electrodeposition of transition metals on the silicon wafers used here. We would also like to thank Peter Sheldon of NREL for his support of the technique development work. This work was funded by the U. S. Department of Energy under contract # DE-AC36-83CH10093.

## References

[1.] R. K. Ahrenkiel, *Solar Cells and* Solar Energy Materials (in press).
[2.] Ahrenkiel, R.K., Johnston, S.W., *Solar Cells and Solar Energy Materials*, **55**, pp. 59-73 (1998).
[3.] Ahrenkiel, R.K., Johnston, S.W., *Mat. Res. Soc. Symp. Proc.,* Materials Research Society, **510**, pp. 575-581 (1998).
[4.] U. S. Patent 5,929,652, Richard Ahrenkiel, July 27, 1999.
[5.] U. S. Patent 6,275,06 Richard Ahrenkiel and Steven Johnston, August 14, 2001
[6.] U. S. Patent 6,369,603, Steven Johnston and Richard Ahrenkiel, April 9, 2002.
[7.] M'Saad, H., Michel, J., Lappe, J.J., Kimerling, L.C., *J. Electronic Materials*, **23**, p. 487 (1994).
[8.] Bube, R.H. *Photoelectric Properties of Semiconductors*, Cambridge University Press, New York, p. 20 (1992).